MODEL STUDIES ON SEISMIC GROUND MOTIONS IN A DIPPING LAYER

M. Ohtsu (I)
S. Hirose (II)
Y. Niwa (III)
Presenting Author : M. Ohtsu

SUMMARY

Seismic ground motions in a dipping layer were investigated by model studies. Elastic waves propagating through dipping layer models were detected by using the acoustic emission (AE) monitoring system. Detected waveforms were simulated by the boundary integral equation (BIE) method. Those were also compared with waveforms based on the ray theory. The results showed that the detected waveforms were in good agreement with the waveforms computed by the BIE method.

Frequency responses of dipping layer models were determined on the basis of the linear system theory. Those spectral responses reproduced an essential feature of analytical results computed by the BIE method.

INTRODUCTION

The geological structure with a dipping layer represents the model of the continental boundary region, or the sediment-filled valley and bed rock system. Propagating through this structure, elastic waves are scattered in the layer, where reflected and diffracted waves are generated. To clarify the complicated effect of a dipping layer on seismic ground motions, we carried out model studies experimentally by use of the acoustic emission (AE) monitoring system, and analytically by use of the boundary integral equation (BIE) method.

A sudden release of stored elastic energy generates an elastic wave, when materials deform and/or fracture. The transient wave emission phenomenon or the emitted wave itself caused by a release of energy is defined as AE. From this point of view, the source characterization of AE is not much different from the focal mechanism of earthquake (Ref. 1). Therefore, the AE method may provide a promise of the study of focal mechanisms by detecting AE signals due to microfracturing (Ref. 2). We applied the Knopoff-De Hoop representation theorem to study source mechanisms of AE, and simulated AE waveforms (Ref. 3).

In the present report, we employed the AE monitoring system to detect elastic waves diffracted in a dipping layer model, instead of investigating

(I) Assistant professor of Civil Engineering, Kumamoto University, Kumamoto, JAPAN

(II) Instructor of Civil Engineering, Kyoto University, Kyoto, JAPAN

(III) Professor of Civil Engineering, Kyoto University, Kyoto, JAPAN

relations between source mechanisms and wave motions of AE (Ref. 4). The AE monitoring system is more sensitive and detects broader frequency components than the ordinary accelerometer system. This implies that we can investigate characteristics of earthquakes from short period components to long period components easily in model studies.

Since phenomena of wave scattering in irregular surfaces and interfaces give rise to locally distributed seismic risk, the effects of various topography and geologic structures on ground motions have been studied by several methods of numerical analyses (Ref. 5), such as FEM, FDM, Aki-Larner's method, and the ray theory etc. (Ref. 6). Taking an analytical feasibility for the transient wave problem into consideration, we employed the BIE method (Ref. 7) to compare experimental results with analytical results.

EXPERIMENTAL PROCEDURE

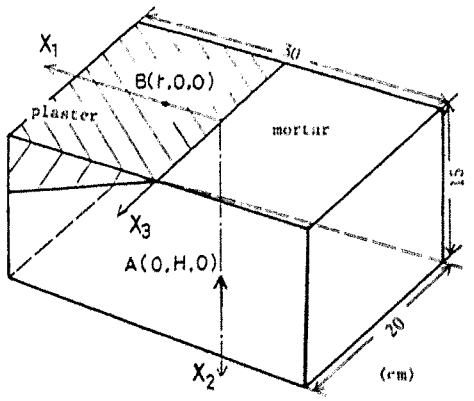

Fig. 1 A sketch of the dipping layer model.

Fig. 1 shows an example of specimens employed for the dipping layer model. Model specimens were made of mortar and plaster, which correspond to a bed rock and a dipping layer, respectively. Dipping angle θ_d of the layer was varied from 10° to 45°. A mass density of mortar was 2.073 and P-wave velocity of mortar c_p was measured as 3919 m/sec. A ratio between mass densities of mortar and plaster was 1.332, and that between P-wave velocities was 1.896. Poisson's ratios of both materials were 0.2.

The monitoring system consists of AE transducers, a bandpass filter selected for 10 kHz - 300 kHz, and an amplifier unit with 60 dB total gain. Fig. 2 shows the block diagram of the monitoring and recording system. The piezoelectric AE transducer (NF Circuit Block, Tokyo, Model 905S) was attached at point A as shown in Fig. 1 on the lower surface of the model and an electric step pulse was charged to the transducer. The rise time of the step pulse was less than 3 nsec (10^{-9} sec) and the voltage was approximately 1V. It produced a transient point force f(t). Elastic waves generated by point

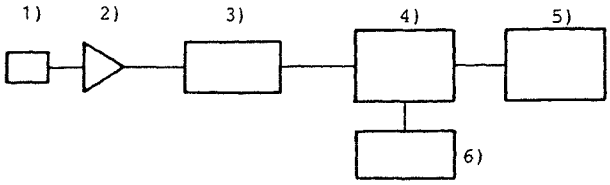

1) AE transducer
2) Pre-amplifier (20dB gain, 10kHz high-pass)
3) Discriminator (40dB gain, 300kHz low-pass)
4) Transient recorder
5) Digital cassette tape unit
6) Oscilloscope

Fig. 2 A block diagram of the AE monitoring and recording system.

force traveled within the model and were detected at point B in Fig. 1 by another transducer on the upper surface, after diffracted and reflected waves were generated in the dipping layer of plaster.

Transient elastic waves within a few μsec after a first arrival were filtered, amplified, and recorded onto digital-cassette tape at the 10 MHz sampling frequency, because the latter portion of the detected waveform consisted of reflections from the outer surface of the model.

The signal flow system is shown schematically in Fig. 3. If all system components are considered as linear, the output is expressed in the time domain and the frequency domain, as follows:

$$o(t)=w_u(t)*w_t(t)*w_m(t)*f(t), \tag{1}$$

$$O(f)=W_u(f)W_t(f)W_m(f)F(f), \tag{2}$$

where * denotes a convolution integral. O(f), W(f), and F(f) correspond to Fourier transforms of o(t), w(t), and f(t), respectively. Derivation of equations (1) and (2) is based on the linear system theory. Characteristics of the transfer functions in these equations are discussed later.

NUMERICAL ANALYSIS

In numerical analyses, we regarded a spherical wave generated by point force in the experiments as a plane wave because of a simplification of the problem.

Fig. 4 shows the dipping layer model for the numerical analyses. In this figure, domains D_1 and D_2 correspond to a dipping layer and a bed rock, respectively. Both domains consist of isotropic, homogeneous, linear elastic solids and they are in the plane strain state. Boundaries S_1 and S_3 represent stress free surfaces. Displacement components and stress tractions are referred to as continuous on boundary S_2. And the incident P-wave im-

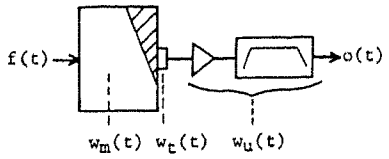

f(t) : point force

$w_m(t)$: transfer function of the model

$w_t(t)$: transfer function of the transducer

$w_u(t)$: transfer function of the amplifier and filter unit

o(t) : output

Fig. 3 The signal flow process.

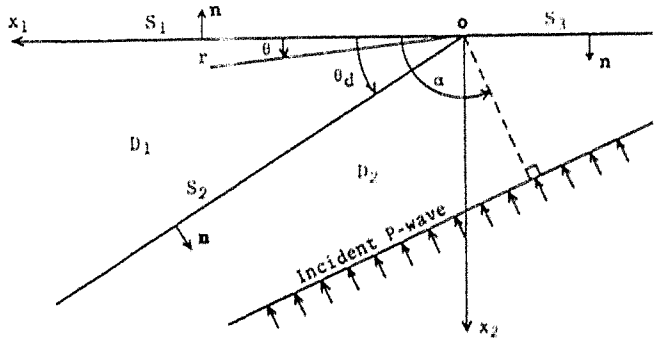

Fig. 4 The dipping layer model.

plies the elastic wave generated by point force in the experiments. The plane wave incident on boundary S_2 reflects several times in the dipping layer and propagates downward without further collisions with boundaries.

Taking account of the boundary conditions, we constructed the BIE and calculated the displacement on a free surface due to the incident P-wave. We solved numerically in the frequency domain by use of the steady state solution of Green's function (Ref. 7). The transient solution of displacement due to the incident P-wave in the time domain was obtained by applying the inverse Fourier transform to the solution in the frequency domain. The fast Fourier transform (FFT) was employed in this calculation. Since this procedure is already discussed (Ref. 8), we do not repeat it here, except some remarks on the computation.

In the numerical evaluation of the boundary integral, we substitute a finite integral path for a semi-infinite integral path on a half space boundary, after investigating the effect of path length on numerical results. Although the stress traction may have singularity at the origin O in Fig. 4, we did not apply a higher order approximation to displacement components at this point. Because it is known that the effect of singularity at a vertex of the dipping layer is inconsequential for ground motions on a free surface except at the vicinity of a vertex.

We also calculated the transient displacement on a free surface as the sum of each ray, which was obtained by the same procedure as in Ref. 6 on the basis of the ray theory.

RESULTS AND DISCUSSION

Detected waves were simulated analytically in the time domain. In this case, we required information of each transfer function w(t) and an applied force f(t) in Fig. 3. Those are already known by the previous study (Ref. 9), as follows:

1) Frequency response $W_u(f)$ represents a flat response in the observed frequency range 10 kHz - 300 kHz.

2) Since physical quantities of elastic waves detected by the transducer employed are considered as vertical accelerations at a free surface, $w_t(t)$ is assumed to be a second order differential operator.

3) The spherical P-wave generated by point force f(t) is regarded as incident plane wave i(t). That is approximated by the following function,

$$d^2i(t)/dt^2=(a-0.5)e^{-a}$$

where $a = (\pi t/t_p)^2$ and $t_p = 7.4$ μsec.

From the preliminary tests, we knew that S-wave and reflected waves from the outer boundary arrived at the observation point after 30 μsec elapsed from the P-wave arrival time. Therefore, we computed wave motions due to incident P-wave, by use of the BIE method and the ray theory. Fig. 5 a) shows an example of detected waveforms in the experiments, while Fig. 5 b) shows corresponding simulated waveforms. In Fig. 5 b), the solid curve represents the acceleration waveform computed by the BIE method and the dashed curve represents that of the ray theory. The precise ratio of electro-mechanical conversion is unknown, so that vertical scales of two figures are relative. Furthermore the time of initial wave motions in Fig. 5 a) is meaningless, because it depends on the triggering of the transient recorder. In Fig. 5 a), saturation of amplitude is seen at about 35 μsec after the first arrival. This corresponds to the arrival time of reflected waves from the outer boundary of the model. A comparison between the detected wave and the simulated waves shows that the detected waveform is in good agreement with the computed waveform by the BIE method. We know that a discrepancy between solutions obtained by the BIE method and by the ray theory results from the effect of refracted waves induced by the diffracted wave, which propagates along boundary S_2 in Fig. 4 (refer to our another report on theoretical analysis). Consequently, these figures imply that the diffracted wave was generated in the model specimen. In the numerical analyses, we regarded the model as the two-dimensional problem. The results of simulation analyses show that our simplification of the problem was appropriate. It also provides a feasibility of model studies by using the AE monitoring system experimentally and the BIE method analytically.

To investigate the frequency response of the dipping layer structure, the detected waves were also analyzed in the frequency domain. In the experiments, we employed the other model besides the dipping layer model. Detecting wave motions in these two models by use of the same monitoring system, the

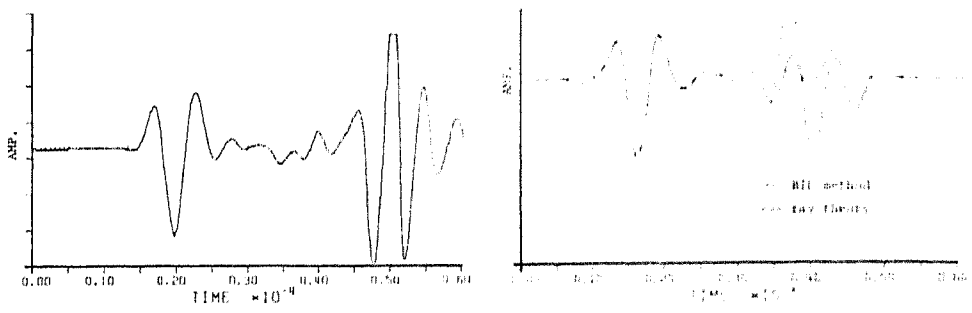

a) b)

Fig. 5 a) The detected waveform and b) the simulated waveform at point B (r = 4 cm) for the case of dipping angle Θ_d = 30° and normal incident of P-wave to a free surface.

frequency response $W_m(f)$ of the dipping layer model was calculated on the basis of the linear system theory from equation (2), as follows:

$$W_m(f)=W_m'(f)O(f)/O'(f) \tag{3}$$

where $W_m'(f)$ and $O'(f)$ denote the Fourier transforms of the transfer function and the output signal of the other model. Because common factors of transfer functions in the signal flow system are cancelled out, characteristics of $W_t(f)$, $W_u(f)$, and $F(f)$ are inconsequential in equation (3). This implies that we can employ any kinds of monitoring devices in this analysis. We used a mortar block of dimensions of 30 cm x 15 cm x 20 cm as the other model, whose frequency response $W_m'(f)$ was considered as flat. Then we compared the frequency response $W_m(f)$ obtained from equation (3) with analytical results obtained by the BIE method and the ray theory. Analytical results were calculated by the Fourier transform of the simulated waveforms.

Fig. 6 a) and b) show $W_m(f)$ obtained from equation (3) and from analytical results. In these figures, the abscissa shows the normalized non-dimensional frequency ($x_1 f/c_p$). It is seen that the spectral curve determined experimentally reproduces an essential feature of the analytical result obtained by the BIE method. This shows a promise to determine the frequency response of the dipping layer by model studies.

CONCLUDING REMARKS

We employed the AE monitoring system to investigate seismic ground motions in the dipping layer model, and compared detected waves with analytical results. Taking an analytical feasibility for transient wave problem in a half space into consideration, we used the BIE method and the ray theory in

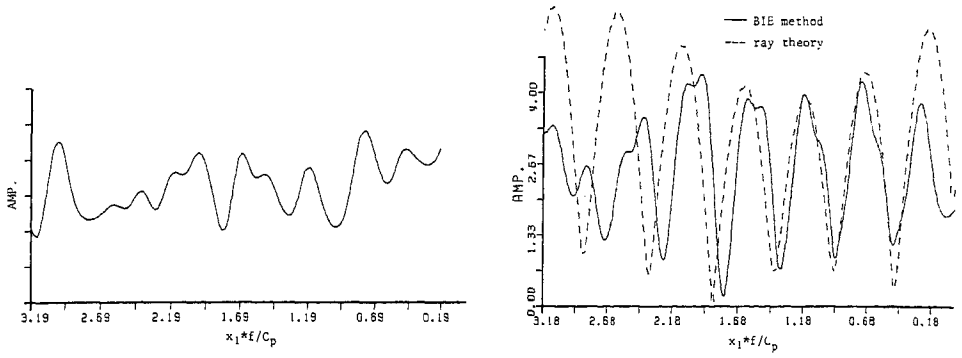

a) b)

Fig. 6 Frequency responses obtained from a) the experiment and b) the analytical results for the case of dipping angle $\theta_d = 30^\circ$ and incident angle $\alpha = 120^\circ$.

the numerical analyses. Analyses in both the time domain and the frequency domain were carried out. In this case, we regarded a spherical wave due to point force in the experiments as a plane wave. We assumed that domains to be analyzed consisted of isotropic, homogeneous, linear elastic solids and they were in the plane strain state.

In spite of these simplifications of the problem, the waveforms computed by the BIE method were in good agreement with the detected waveforms by the AE monitoring system. These results imply that wave diffractions were observed in the model specimens employed here. And an applicability of the BIE method to the diffracted wave problem in a dipping layer is shown.

The frequency responses of dipping layer models were obtained on the basis of the linear system theory. The response curves reproduced an essential feature of the analytical results obtained by the BIE method. This shows a promise to determine frequency responses of complicated geological structures by model studies.

REFERENCES

1. Mogi, K., " Earthquakes as acoustic emission - 1980 Izu Peninsular earthquake in particular," Journal of Acoustic Emission, Vol.1, No.1, 37 - 44, 1982.
2. Scholz, C. H., " The frequency - magnitude relation of microfracturing in rock and its relation to earthquakes," Bull. Seism. Soc. Am., Vol. 58, No.1, 399 - 415, 1968.
3. Ohtsu, M., " Theoretical treatment of acoustic emission and source mechanisms in concrete," Memoirs of the Faculty of Engineering, Kumamoto University,

Vol. 47, No. 2, 1 - 21, 1982.
4. Ohtsu, M., " Source mechanism and waveform analysis of acoustic emission in concrete," Journal of Acoustic Emission, Vol. 1, No. 2, 103 - 112, 1982.
5. Aki, K. and P. G. Richards, Quantitative seismology theory and methods, Vol. II, Chap. 13, W. H. Freeman and Company, San Francisco, 1980.
6. Ishii, H. and R. M. Ellis, " Multiple reflection of plane P and SV waves by a dipping layer," Geophy. J. R. astr. Soc., Vol. 20, 11 - 30, 1970.
7. Kupraze, V. D., Potential methods in the theory of elasticity, Israel Program for Scientific Translations, Jerusalem, 1965.
8. Niwa, Y., M. Ohtsu and S. Hirose, " Seismic analysis for a dipping layer," Proc. 6th Japan Earthq. Eng. Symp., 417 - 424, 1982.
9. Niwa, Y., S. Kobayashi and M. Ohtsu, " Source mechanisms and wave motions of acoustic emission in rock-like materials," 3rd Conference AE/MA in Geologic Structures and Materials, The Pennsylvania State University, 1981.